Biophysical *Journal*
Biophysical Letter

Biophysical Society

Functional Validation of Heteromeric Kainate Receptor Models

Teresa Paramo,[1] Patricia M. G. E. Brown,[2] Maria Musgaard,[1] Derek Bowie,[3] and Philip C. Biggin[1,*]
[1]Department of Biochemistry, University of Oxford, Oxford, United Kingdom; [2]Integrated Program in Neurosciences and [3]Department of Pharmacology and Therapeutics, McGill University, Montréal, Québec, Canada

ABSTRACT Kainate receptors require the presence of external ions for gating. Most work thus far has been performed on homomeric GluK2 but, in vivo, kainate receptors are likely heterotetramers. Agonists bind to the ligand-binding domain (LBD) which is arranged as a dimer of dimers as exemplified in homomeric structures, but no high-resolution structure currently exists of heteromeric kainate receptors. In a full-length heterotetramer, the LBDs could potentially be arranged either as a GluK2 homomer alongside a GluK5 homomer or as two GluK2/K5 heterodimers. We have constructed models of the LBD dimers based on the GluK2 LBD crystal structures and investigated their stability with molecular dynamics simulations. We have then used the models to make predictions about the functional behavior of the full-length GluK2/K5 receptor, which we confirmed via electrophysiological recordings. A key prediction and observation is that lithium ions bind to the dimer interface of GluK2/K5 heteromers and slow their desensitization.

GluK2 and GluK5 are the most widely expressed kainate receptor subunits in the central nervous system (CNS) (1,2). In coexpressing cells, they form GluK2/K5 heterotetramers with a 2:2 stoichiometry (3), exhibiting distinct functional and pharmacological properties, which differ significantly from the more studied GluK2 homotetramer (2,4). For example, the presence of the GluK5 subunit in the receptor increases the sensitivity to agonists such as glutamate (5) or kainate (2), and provides an increased response to α-amino-3-hydroxy-5-methyl-4-isoxazolepropionic acid (AMPA) (2). Thus, despite belonging to the same family, GluK5 possesses unique features that help to broaden the functional and pharmacological profile of kainate receptors, which have been identified as a potential target for the treatment of mood disorders, epilepsy, and pain perception (6). Indeed, GluK2/K5 receptors play a major role in chronic and recurrent seizures in temporal lobe epilepsy (7).

Despite their inability to form functional homomeric channels, the secondary subunits, GluK4 and GluK5, are important at synapses and the ablation of the genes encoding these subunits in mice leads to the complete suppression of the synaptic kainate receptor-mediated currents (8). This suggests that heteromeric complexes including these two subunits are essential for the ionotropic function of the kainate receptors in vivo, and thus an atomically detailed model of the heteromer, particularly at the level of the ligand-binding domains (LBDs), would be very useful in furthering our understanding of these receptors. Unfortunately, despite the in vivo relevance of the GluK2/K5 heterotetramer (8), experimental difficulties in dealing with heterogeneity have hindered the determination of its structural arrangement so far. Given the high structural similarity among ionotropic glutamate receptors (iGluRs), one would expect a GluK2/K5 heteromer to share the commonly observed symmetry mismatch between the extracellular domain, which arranges as a dimer of dimers, and the fourfold symmetric transmembrane domain (9–13). Despite such overall structural similarity, there is growing evidence that minor changes in composition can have dramatic influences on function, and therefore any similarities should be extrapolated with caution. In particular, a series of point mutations at the dimer interface of the LBDs have been shown to alter the receptor kinetics by either delaying the onset of desensitization (14,15) or even disrupting the gating of the receptor (16).

However, functional effects provide an opportunity to validate a potential model of GluK2/K5. Indeed, as with any model, the usefulness can be assessed by its ability to make functional predictions. Here, we present an atomistic model of the LBD dimer of the physiologically relevant GluK2/K5 receptor. The LBDs of iGluRs are useful as a reduced model of receptor gating, as they have been shown

Submitted July 25, 2017, and accepted for publication August 31, 2017.
*Correspondence: philip.biggin@bioch.ox.ac.uk
Editor: Vasanthi Jayaraman.
http://dx.doi.org/10.1016/j.bpj.2017.08.047

to reproduce ligand-binding affinities (17) as well as conserving similar structural features present when part of the full-length receptor (18). Moreover, changes in the interfacial interactions within LBD dimers (18,19) are believed to drive the receptor state transitions. Additionally, the presence of three monovalent modulatory ions at the LBD interface are key for the stability of the conducting configuration of kainate receptors (20,21). Furthermore, the release of two of these ions from the LBD marks the start of the desensitization process (16) through the separation of the LBD interface (9,11).

In this study, we show how initial structural stability assessment of potential LBD combinations suggests that the LBDs are most likely comprised of GluK2/K5 heterodimers and that this model can predict an effect of Li^+ on the desensitization properties of the full-length receptor. The effects of Li^+ were confirmed by electrophysiological recordings. The foremost uncertainty regarding the structure of the GluK2/K5 heteromers is the LBD composition itself. Although some experimental data suggest that the heterotetrameric receptor might be composed of a dimer of GluK2/K5 heterodimers (22,23), the possibility of a LBD formed by two GluK2 and GluK5 homodimers has not yet been ruled out. Therefore, we generated and assessed models of GluK2/K5 and GluK5/K5 LBDs. Simulations were also compared to simulations of the experimentally resolved GluK2 homodimer structure (19) (see the Supporting Material).

As an initial assessment of structural stability, we monitored the behavior of the individual LBD lobes (D1 and D2) in maintaining a closed-cleft conformation in the presence of glutamate. The D1-D2 distance of the LBD domains has been previously used as a structural marker of iGluR amplitude response (24–26), although we note that it may not linearly correspond to response amplitude (27). It is generally thought that the presence of partial agonists correlates with a lower degree of D1-D2 closure, which could in turn decrease the frequency at which the receptors access the highest conductance states (28). As kainate receptors are known to require ions for function, we performed molecular

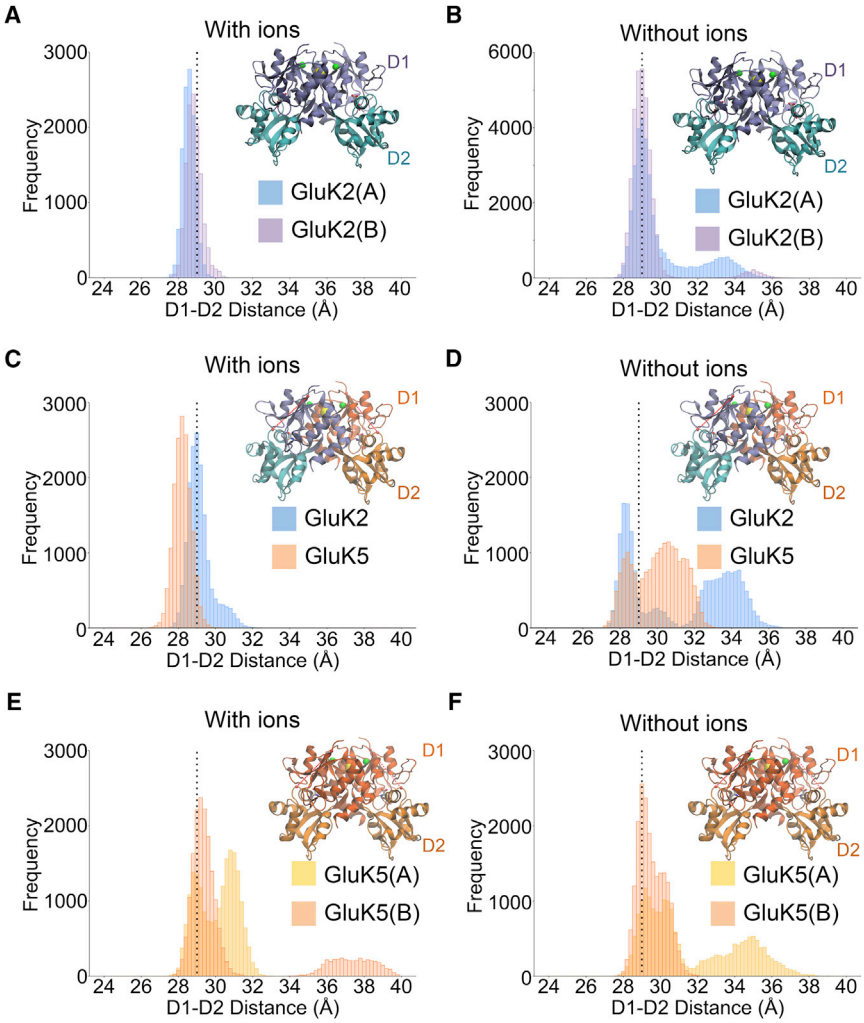

FIGURE 1 D1-D2 distance distributions from the last 20 ns of five independent simulations for the GluK2 homomer (*A* and *B*), the GluK2/K5 heteromer (*C* and *D*), and the GluK5 homomer (*E* and *F*) (additional data for *B* was available for GluK2 without ions from previous simulations (16,34)) in the presence and absence of modulatory sodium (*green spheres*) and chloride (*yellow spheres*) ions. The frequency distributions use 0.2 Å bins. Simulations with ions were manually verified and were omitted from the "with ion" distributions if there was dissociation. The dashed vertical line indicates the equivalent distance in the GluK2 homodimer crystal structure (3G3F) (19). To see this figure in color, go online.

dynamics simulations with and without ions (Na^+ and Cl^-) present. Dimers of GluK2 and GluK2/K5 maintain a gating configuration when the modulatory ions are bound, and move away from that state when the ions are absent (Fig. 1), reflecting loss of stability in terms of cleft closure.

Interestingly, the GluK5 homodimer was unstable both with and without ions, and more likely to exist as an open-cleft conformation (Fig. 1). Although the link between the number of closed clefts and subconductance states is established for AMPA receptors but not for kainate receptors (29), these results tend to support the hypothesis that GluK2/K5 receptors are more likely formed by a dimer of GluK2/K5 heterodimers (4,23,30).

The relevance of ion binding in the gating configuration of the GluK2 homodimer and GluK2/K5 heterodimer became evident in two of the "bound" simulations, where the cations spontaneously unbind from the LBD interface (Fig. S1). In both systems, the release of one of the two cations was followed by the opening of the clamshell of GluK2, an event not observed in any of the simulations in which Na^+ ions remained bound. Of note, the key "anchor" residue, R523, in the binding site (Figs. 2 and S3) is adjacent to E524, which interacts directly with one of the cations, thereby providing a direct link between the dynamics of the interface and the behavior of the binding site (and consequently the stability of the clamshell). Interestingly, several additional hydrogen bonds are formed between glutamate and GluK5, facilitated by the highly conserved (between

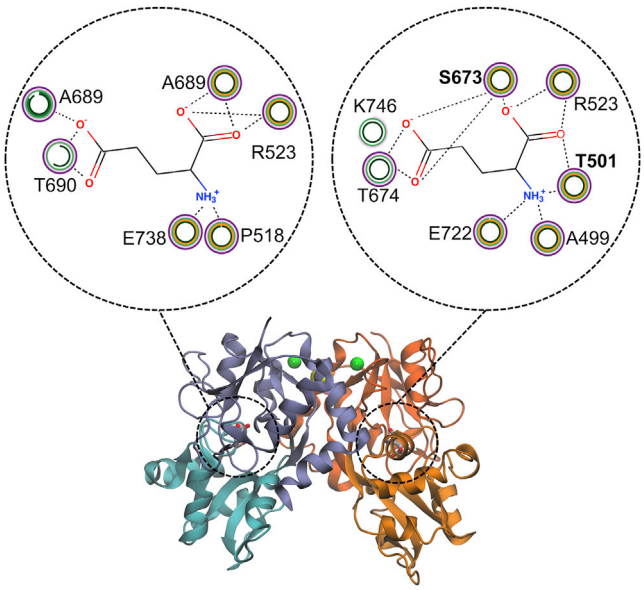

FIGURE 2 Glutamate binding interactions (from the last 20 ns of five repeat simulations) observed in GluK2 and GluK5 within the GluK2/K5 heterodimer, where the dashed line represents a hydrogen bond and the five circular rings indicate the frequency of these interaction within each of the five simulation repeats (*no color* indicates no interaction in that repeat). S673 and T501 (*bold*) contribute additional interactions from the GluK5 subunit. To see this figure in color, go online.

species) residues T501 and S673 (bold in Fig. 2), which are both alanines in GluK2. The higher number of interactions is consistent with the higher binding affinity of GluK5 for glutamate.

Given the requirement of the Na^+ ions for dimer stability, we tested the effect of Li^+ ions on the structural properties of the LBDs following our previous approach for GluK2 homomers (31) and similar to our recent approach to examining desensitization kinetics in AMPA receptors (32). Here, we repeated the simulations of the three LBDs studied, replacing Na^+ with Li^+ in the salt buffer (Fig. 3, *A* and *B*). In our simulations, Li^+ ions remained bound to the LBD. Given the previously documented role of ions at this interface in the process of desensitization, we examined the D1-D1 distances at the dimer interface, between subunits (see Fig. S2 for definitions) for each of the systems (Fig. 3). Several things are noteworthy. Firstly, in the presence of sodium, the D1-D1 equilibrium distance (peak of the histogram) shifts depending on the nature of the dimer composition (Fig. 3 *A*).

Specifically, the GluK2/K5 distance is increased (to 15.4 Å) and the GluK5/K5 distance is even further increased to 16.2 Å (Fig. 3 *A*). In the presence of Li^+, (Fig. 3 *B*), the GluK2/K2 distribution is broader and centered at a higher separation when compared to Na^+. In contrast, the separations for the GluK2/K5 and GluK5/K5 dimers are reduced compared to the distances observed in the presence of Na^+; the values were in fact similar to those observed in the GluK2/K2 crystal structure (19). Since the distances here have previously been linked to receptor desensitization in GluK2 homomers (16), this suggested to us that the presence of Li^+ in GluK5-containing receptors should result in slower desensitization. To test this, we studied the rates of desensitization for recombinantly-expressed GluK2 and GluK2/K5 using outside-out patches (see Supporting Material). As previously shown (33), the decay kinetics of GluK2 responses were accelerated in the presence of LiCl (Fig. 3 *C*). Interestingly, GluK2/K5 decay kinetics were slowed by more than threefold in LiCl (Fig. 3, *D* and *E*). These results are in agreement with the simulation data and suggest that, similar to AMPA receptors, the stability of the LBD dimer interface of GluK2/GluK5 regulates desensitization kinetics (Fig. 3, *C*–*E*). It will be interesting to see the effects, if any, of other cations on GluK5.

To ascertain the thermodynamic impact of Li^+ on the LBD of the heterotetramer, we calculated the free energy of binding (affinity) of Na^+ and Li^+ in both the GluK2 homodimer and the GluK2/K5 heterodimer using free energy perturbation, as previously described (31). The results showed that although both systems preferably bind to Li^+, a ~3 kcal/mol higher affinity is observed in the heterodimer (see Table S1 for details). Such a difference suggests that the tighter packing of the D1-D1 segments of the GluK2/K5 LBD in the presence of Li^+ (Fig. 3 *B*) could result in a higher energy barrier to be overcome during the D1-D1 separation

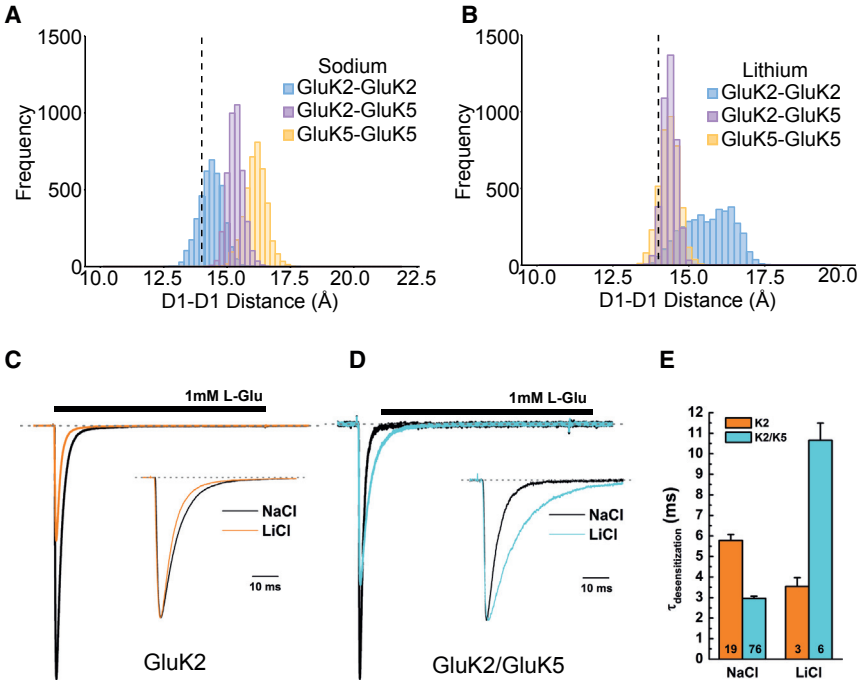

FIGURE 3 Sodium stabilizes GluK2 homomer models (*A*) but lithium does not (*B*). Lithium does, however, stabilize GluK2/K5 heteromer models. Recordings in the presence of different cations for the GluK2 homomer and GluK2/K5 heteromer show different responses (*C* and *D*). Example electrophysiological traces showing responses in NaCl (*black*) and LiCl (*orange/cyan*) background (GluK2 (*C*), GluK2/K5 (*D*)). Insets show peak-normalized responses to highlight changes in decay kinetics. (*E*) Analysis of the fast exponential decay component (τ_{fast}) for GluK2 and GluK2/K5 in NaCl and LiCl background. Bars indicate the mean and error bars are mean ± SE; the number of patches is shown on each bar. To see this figure in color, go online.

movements that are believed to trigger desensitization. The mechanism with which Li^+ ions exert their effect on GluK2/K5 heteromers appears to result from tighter interface packing compared to when Na^+ ions are present. Indeed, the solvent density across the different systems is smaller in the presence of Li^+ (Fig. S3). In GluK5-containing models, there is a smaller volume of water density accessible to the ions and the Li^+ appears to mediate more cross-dimer interactions. The distribution of direct water-cation interactions also supports this (Fig. S4). These observations are in agreement with our previous studies examining the dynamic behavior of this interface (16,32,34).

SUPPORTING MATERIAL

Supporting Materials and Methods, four figures, and one table are available at http://www.biophysj.org/biophysj/supplemental/S0006-3495(17)30970-0.

AUTHOR CONTRIBUTIONS

D.B. and P.C.B. designed the research. T.P., M.M., and P.M.G.E.B. performed the research and analyzed the results. T.P. and P.C.B. wrote the article.

ACKNOWLEDGMENTS

We thank L. Domicevica, G. Gerogiokas, and M.R.P. Aurousseau for discussions.

T.P. was funded by the Medical Research Council (MRC) (MR/M000435/1), M.M. by the Alfred Benzon Foundation, P.M.G.E.B. by the Fonds de Recherche en Santé du Québec, and D.B. by the Canadian Institutes of Health Research. We thank the Advanced Research Computing facility, the Engineering and Physical Sciences Research Council (EPSRC) National Service for Computational Chemistry Software (NSCCS) (EP/J003921/1), and the ARCHER UK National Supercomputing Services for computer time granted via the High-End Computing Consortium for Biomolecular Simulation (http://www.hecbiosim.ac.uk), supported by the EPSRC (EP/L000253/1). Work in the P.C.B. laboratory is supported by the Biotechnology and Biological Sciences Research Council and the MRC.

REFERENCES

1. Petralia, R. S., Y.-X. Wang, and R. J. Wenthold. 1994. Histological and ultrastructural localization of the kainate receptor subunits, KA2 and GluR6/7, in the rat nervous system using selective antipeptide antibodies. *J. Comp. Neurol.* 349:85–110.
2. Herb, A., N. Burnashev, …, P. H. Seeburg. 1992. The KA-2 subunit of excitatory amino acid receptors shows widespread expression in brain and forms ion channels with distantly related subunits. *Neuron.* 8:775–785.
3. Reiner, A., R. J. Arant, and E. Y. Isacoff. 2012. Assembly stoichiometry of the GluK2/GluK5 kainate receptor complex. *Cell Reports.* 1:234–240.
4. Fisher, J. L., and D. D. Mott. 2011. Distinct functional roles of subunits within the heteromeric kainate receptor. *J. Neurosci.* 31:17113–17122.
5. Barberis, A., S. Sachidhanandam, and C. Mulle. 2008. GluR6/KA2 kainate receptors mediate slow-deactivating currents. *J. Neurosci.* 28:6402–6406.
6. Lerma, J., and J. M. Marques. 2013. Kainate receptors in health and disease. *Neuron.* 80:292–311.
7. Crépel, V., and C. Mulle. 2015. Physiopathology of kainate receptors in epilepsy. *Curr. Opin. Pharmacol.* 20:83–88.
8. Fernandes, H. B., J. S. Catches, …, A. Contractor. 2009. High-affinity kainate receptor subunits are necessary for ionotropic but not metabotropic signaling. *Neuron.* 63:818–829.

9. Meyerson, J. R., J. Kumar, …, S. Subramaniam. 2014. Structural mechanism of glutamate receptor activation and desensitization. *Nature.* 514:328–334.
10. Karakas, E., and H. Furukawa. 2014. Crystal structure of a heterotetrameric NMDA receptor ion channel. *Science.* 344:992–997.
11. Dürr, K. L., L. Chen, …, E. Gouaux. 2014. Structure and dynamics of AMPA receptor GluA2 in resting, pre-open, and desensitized states. *Cell.* 158:778–792.
12. Sobolevsky, A. I., M. P. Rosconi, and E. Gouaux. 2009. X-ray structure, symmetry and mechanism of an AMPA-subtype glutamate receptor. *Nature.* 462:745–756.
13. Lee, C. H., W. Lü, …, E. Gouaux. 2014. NMDA receptor structures reveal subunit arrangement and pore architecture. *Nature.* 511:191–197.
14. Zhang, Y., N. Nayeem, …, T. Green. 2006. Interface interactions modulating desensitization of the kainate-selective ionotropic glutamate receptor subunit GluR6. *J. Neurosci.* 26:10033–10042.
15. Nayeem, N., O. Mayans, and T. Green. 2013. Correlating efficacy and desensitization with GluK2 ligand-binding domain movements. *Open Biol.* 3:130051.
16. Dawe, G. B., M. Musgaard, …, D. Bowie. 2013. Defining the structural relationship between kainate-receptor deactivation and desensitization. *Nat. Struct. Mol. Biol.* 20:1054–1061.
17. Kuusinen, A., M. Arvola, and K. Keinänen. 1995. Molecular dissection of the agonist binding site of an AMPA receptor. *EMBO J.* 14:6327–6332.
18. Traynelis, S. F., L. P. Wollmuth, …, R. Dingledine. 2010. Glutamate receptor ion channels: structure, regulation, and function. *Pharmacol. Rev.* 62:405–496.
19. Chaudhry, C., M. C. Weston, …, M. L. Mayer. 2009. Stability of ligand-binding domain dimer assembly controls kainate receptor desensitization. *EMBO J.* 28:1518–1530.
20. Plested, A. J. R., R. Vijayan, …, M. L. Mayer. 2008. Molecular basis of kainate receptor modulation by sodium. *Neuron.* 58:720–735.
21. Bowie, D. 2002. External anions and cations distinguish between AMPA and kainate receptor gating mechanisms. *J. Physiol.* 539:725–733.
22. Kumar, J., P. Schuck, and M. L. Mayer. 2011. Structure and assembly mechanism for heteromeric kainate receptors. *Neuron.* 71:319–331.
23. Reiner, A., and E. Y. Isacoff. 2014. Tethered ligands reveal glutamate receptor desensitization depends on subunit occupancy. *Nat. Chem. Biol.* 10:273–280.
24. Krintel, C., K. Frydenvang, …, J. S. Kastrup. 2014. L-Asp is a useful tool in the purification of the ionotropic glutamate receptor A2 ligand-binding domain. *FEBS J.* 281:2422–2430.
25. Lau, A. Y., and B. Roux. 2011. The hidden energetics of ligand binding and activation in a glutamate receptor. *Nat. Struct. Mol. Biol.* 18:283–287.
26. Armstrong, N., and E. Gouaux. 2000. Mechanisms for activation and antagonism of an AMPA-sensitive glutamate receptor: crystal structures of the GluR2 ligand binding core. *Neuron.* 28:165–181.
27. Fay, A.-M. L., C. R. Corbeil, …, D. Bowie. 2009. Functional characterization and in silico docking of full and partial GluK2 kainate receptor agonists. *Mol. Pharmacol.* 75:1096–1107.
28. Jin, R., T. G. Banke, …, E. Gouaux. 2003. Structural basis for partial agonist action at ionotropic glutamate receptors. *Nat. Neurosci.* 6:803–810.
29. Smith, T. C., and J. R. Howe. 2000. Concentration-dependent substrate behavior of native AMPA receptors. *Nat. Neurosci.* 3:992–997.
30. Fisher, J. L. 2014. The neurotoxin domoate causes long-lasting inhibition of the kainate receptor GluK5 subunit. *Neuropharmacology.* 85:9–17.
31. Vijayan, R., A. J. R. Plested, …, P. C. Biggin. 2009. Selectivity and cooperativity of modulatory ions in a neurotransmitter receptor. *Biophys. J.* 96:1751–1760.
32. Dawe, G. B., M. Musgaard, …, D. Bowie. 2016. Distinct structural pathways coordinate the activation of AMPA receptor-auxiliary subunit complexes. *Neuron.* 89:1264–1276.
33. Wong, A. Y. C., A.-M. L. Fay, and D. Bowie. 2006. External ions are coactivators of kainate receptors. *J. Neurosci.* 26:5750–5755.
34. Musgaard, M., and P. C. Biggin. 2016. Steered molecular dynamics simulations predict conformational stability of glutamate receptors. *J. Chem. Inf. Model.* 56:1787–1797.

Biophysical Journal, Volume *113*

Supplemental Information

Functional Validation of Heteromeric Kainate Receptor Models

Teresa Paramo, Patricia M.G.E. Brown, Maria Musgaard, Derek Bowie, and Philip C. Biggin

Supplemental Information

Functional Validation of Heteromeric Kainate Receptor Models.

T. Paramo,* P.M.G.E. Brown,[†‡] M. Musgaard,* D. Bowie,[‡] and P.C. Biggin*

*Department of Biochemistry, University of Oxford, South Parks Road, Oxford, OX1 3QU; [†]Integrated Program in Neurosciences, McGill University, Montréal, Québec, H3G 0B1; [‡]Department of Pharmacology and Therapeutics, University, Montréal, Québec, H3G 0B1

Address reprint requests and inquiries to Philip.biggin@bioch.ox.ac.uk

Detailed Methods

Model generation

Models of the GluK2/GluK5 heterodimer and GluK5 homodimer LBDs were generated with Modeller (1) using the crystal structure of the GluK2 homodimer (2) (PDB: 3G3F, resolution 1.38 Å) as a template. This structure contains the commonly used polypeptide hydrophilic linker GT between the S1 and S2 segments constituting the LBD, as it has been shown to allow the isolated LBD to reproduce ligand binding affinities (3) associated with the full-length receptor (4). The quality of the generated models was initially assessed with the molpdf and DOPE scoring functions of Modeller, in combination with the stereochemical analysis performed by PROCHECK (5). The best five models were retained for an absolute structural assessment using the QMEAN server (6). All the models selected had a QMEAN Z-score of ~0.7, indicating the quality of the models is comparable to that of experimental structures (7). The best homodimer and heterodimer models were then selected for production simulations, while the second and third best models of each system were used as a control to evaluate simulation reproducibility (see below). Finally, the modulatory ions, glutamate and crystallographic water molecules present in the structure of GluK2 homodimer were added to the models by structural superposition using the STAMP (8) plugin for pair-wise structural alignment available in VMD (9).

Molecular dynamics simulations

Five replicas of 100 ns were simulated for both the GluK5 homodimer and GluK2/GluK5 heterodimer models in the presence and absence of modulatory ions, respectively, accounting for a total of 2 μs simulation sampling. Additionally, we included four 100-500 ns simulation replicas of the GluK2 homodimer from previous studies (10, 11). For each replica, different initial velocities were used to perform an efficient exploration of the conformational space (12). The second and third best models of each system (according to the criteria described in the modelling section) were also simulated under the same conditions to ensure reproducibility of the events observed (see below). All these simulations were performed with GROMACS 5.0.2 (13) using the OPLS all-atom force field (14), which has been previously shown to accurately reproduce thermodynamic and structural properties related to ion binding in kainate receptors (11, 15). The protein dimers were then solvated in a periodic dodecahedral box with the explicit TIP3P water model (16), and subsequently neutralized with a 150 mM concentration of sodium

and chloride ions. Newton's equations of motion were solved with the leap-frog integrator with a time-step of 2 fs, using the LINCS (17) algorithm to constrain the bond lengths. Non-bonded pair lists where updated every 10 steps with a Verlet scheme (18). Van der Waals interactions were switched off at a distance of 1 nm, using a long-range dispersion correction for energy and pressure, while long range electrostatic interactions were calculated using the Particle Mesh Ewald (19) method.

The simulation protocol included the minimization of the models' potential energy with the steepest descent algorithm, followed by a 2 ns solvent equilibration phase imposing position restraints on the protein heavy atoms and crystallographic water and ions. After this equilibration step, production simulations were performed in the *NPT* ensemble, with 300 K temperature and 1 bar isotropic pressure, maintained by the Berendsen thermostat and barostat, respectively (20). The analysis of the simulations was performed using the analysis tools of GROMACS, retaining only the data corresponding to the last 20 ns simulation block unless otherwise stated. Simulations that were with ions were verified by visual inspection. If ions dissociated form the simulation they were not used to calculate the frequency distributions of the "with ions" systems. The analysis of the ion binding site hydration was performed with trj_cavity (21).

Free energy calculations

Relative binding free energies were calculated for the transformation of the two modulatory Na^+ ions into Li^+. To study the convergence of these calculations, forward and reverse transformations were performed for both GluK2 homodimer and GluK2/GluK5 heterodimer systems in presence of the full agonist glutamate. As the charge of the systems was maintained during the transformations, only the van der Waals interactions were decoupled, using eleven equally spaced windows (λ=0.0, 0.1, …, 1.0). Each window was equilibrated following the protocol described above for unbiased simulations, followed by 50 ns production Hamiltonian replica-exchange simulations. These simulations were performed within the NPT ensemble using the Langevin thermostat and the Parrinello-Rahman pressure coupling scheme. Corrections for missing dispersion terms were applied as previously suggested (22). Finally, the results were analyzed with the multiple Bennet-acceptance ratio (MBAR) as implemented in the pymbar software package (23), using the timeseries module (24) to assess the equilibration

time of each window, which was subsequently discarded from the calculation of the free energy differences.

Additional control simulations

To investigate the dependence of our results on the model chosen, we also simulated the 2nd and 3rd best models of the heterodimer, and an additional model of the GluK2 homodimer generated according to the conditions described above. Although in this set of simulations some of the cations spontaneously left the inter-dimeric pocket, the results were consistent with the opening of GluK2 proteins upon ion release (as seen for the simulations derived from the best model – see Fig S1). Thus, the dependency of the presence of modulatory ions to maintain the active configuration of the GluK2-containing dimers is reproducible with different initial models, suggesting the results are robust to this aspect of the initial set up.

Analysis

D1-D2 distances were defined as the distance between the Cα atoms of residues T394 and S652, similar to equivalent measurements in AMPA receptors (25). As in GluA2, these residues are located in each of the S1 and S2 peptide segments, flanking the glutamate-binding site. D1-D1 distances were defined as the difference between the centre of masses of two groups atoms composed by residues Y542, R543, K544, E665, S666 and P667 (GluK2 numbering). The circular "clock" schematics that depict interactions within a binding site were constructed using LINTools (doi: 10.5281/zenodo.45076). Molecular images were generated with the VMD package (9).

Electrophysiological Recordings

Cell Culture and Transfection

HEK293T/17 cells (ATCC) were maintained in minimal essential medium (MEM) containing glutaMAX© supplemented with 10% fetal bovine serum (Invitrogen). Cells were plated at low density ($1.6 - 2.0 \times 10^4$ cells ml^{-1}) on poly-D-lysine-coated 35 mm plastic dishes and were

transiently transfected 24 hours later using the calcium phosphate technique as previously described (26). A GluK2:GluK5 cDNA ratio of 1:10 was used for co-transfections.

Electrophysiology

Experiments were performed 36–48 h after transfection. Agonist solutions were rapidly applied to outside-out patches excised from transfected cells using a piezoelectric stack (Physik Instrumente, Auburn, MA, USA). Solution exchange (10–90% rise time of 250–350 µs) was determined in a separate experiment by measuring the liquid junction current. All recordings were performed using an Axopatch 200B (Molecular Devices, Sunnyvale, CA, USA) using thick-walled borosilicate glass pipettes (3–6 MΩ) coated with dental wax to reduce electrical noise. Current records were filtered at 5 kHz, digitized at 25 kHz and series resistance (3–12 MΩ) was compensated for by 95%. Recordings were performed at holding potentials of -60 mV. Data acquisition was performed using pClamp9 software (Molecular Devices) and tabulated using Microsoft Excel. Experiments were performed at room temperature.

Chemicals were purchased from Sigma-Aldrich (St Louis, MO, USA) unless otherwise indicated. External solutions contained (in mM): 150 NaCl or LiCl, 5 HEPES, 0.1 $MgCl_2$ and 0.1 $CaCl_2$, pH 7.3–7.4. The corresponding hydroxide solutions (NaOH or LiOH) were used to adjust the pH. The internal solution contained (in mM): 115 NaCl, 10 NaF, 5 HEPES, 5 Na_4BAPTA (Life Technologies, Invitrogen, Burlington, ON, Canada), 1 $MgCl_2$, 0.5 $CaCl_2$ and 10 Na_2ATP, pH 7.3–7.4. The osmotic pressure of all solutions was adjusted to 295–300 mOsm with sucrose. Concentrated (100X) L-glutamate stock solutions were prepared by dissolving in the appropriate external solution, adjusting the pH to 7.3–7.4, and stored frozen at −20 °C. Stocks were thawed on the day of the experiment and diluted to a final concentration of 1 mM.

Current responses were fit with multiple exponential functions using Clampfit9 software. Data were illustrated using Origin 7 and Adobe Illustrator.

Figure S1: Evolution of the D1-D2 distance in GluK2 upon release of sodium within a GluK2/K5 dimer. The GluK2/K5 heterodimer is depicted above the graph. The two sodium ions unbind almost simultaneously after 30 ns of simulation (marked in the graph with an asterisk). The absence of sodium ions seems to destabilize the clamshell cleft closure of the GluK2 subunit, which ends up opening ~5 Å from 70 ns of simulation. Within the same timescale, a sodium ion rebinds the sodium binding pocket of GluK5. Sodium and chloride ions are represented by green and yellow spheres respectively.

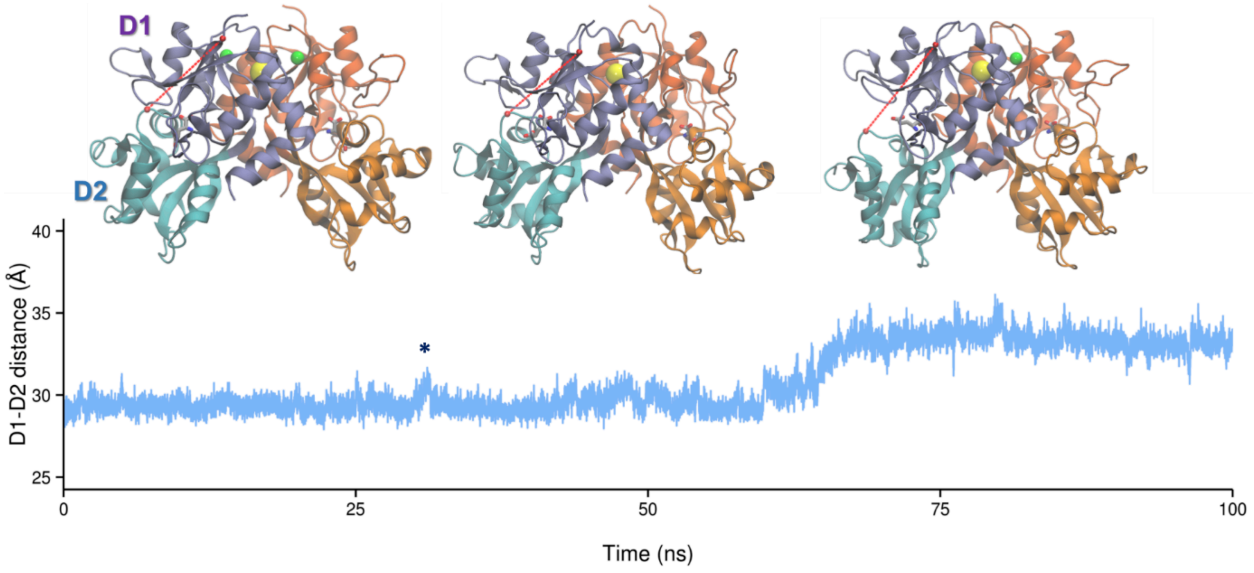

Figure S2: Top view of a GluK2-GluK5 heteromer depicting the D1-D1 distance defined as the distance between the centre of mass of residues Y542, R543, K544, E665, S666 and P667 (GluK2 numbering). GluK2 is in cyan and GluK5 is in orange. Sodium ions are green spheres and the chloride ion is a yellow sphere. Glutamate is shown in liquorice representation in each binding cleft.

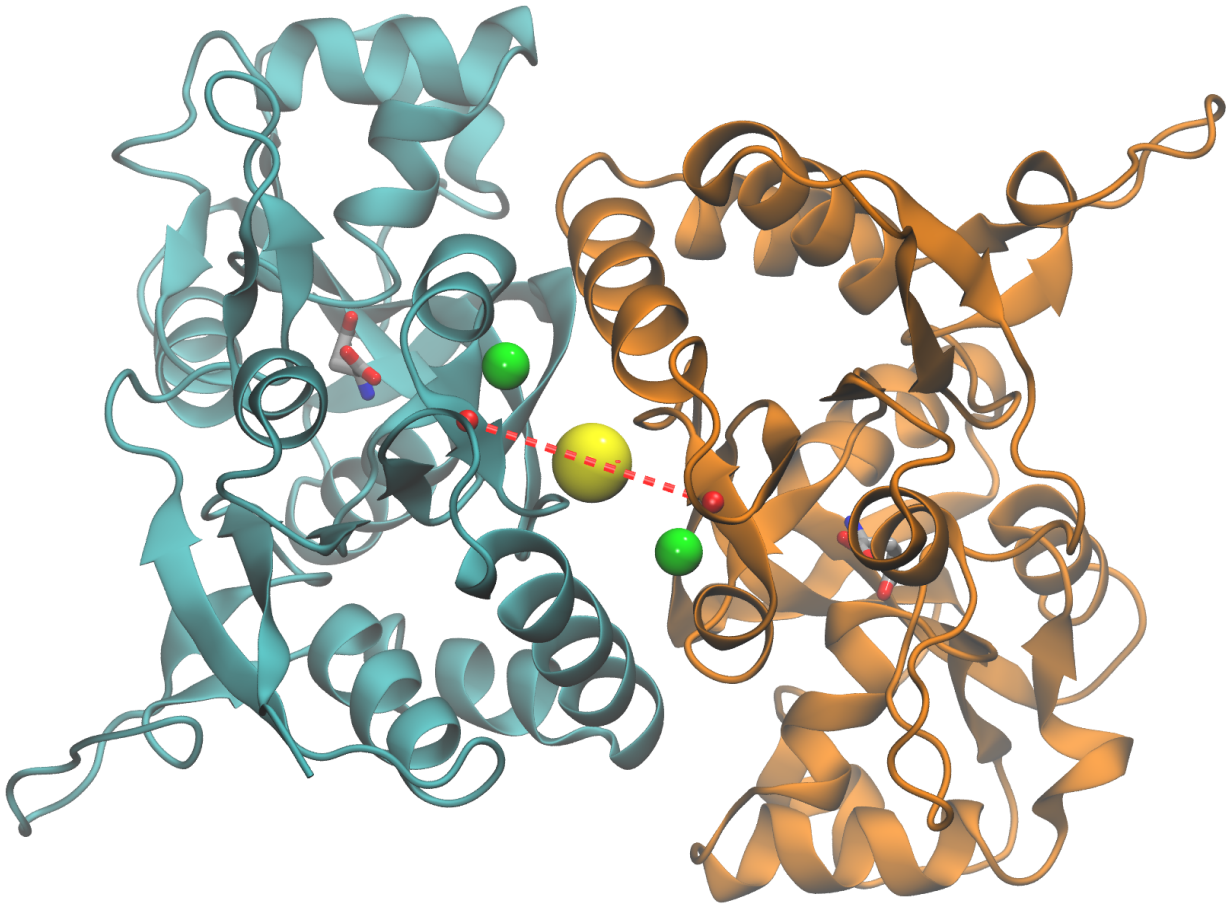

Figure S3: Hydration of the ion-binding pocket. LBDs are depicted as in Fig. 1 of the main manuscript, with key cation-binding residues represented with sticks following the CPK color scheme. The figure shows the last simulation snapshot of the simulations of the GluK2 homodimer (A,D), GluK2-K5 heterodimer (B,E) and GluK5 homodimer (C,F) with Na^+ (green spheres) or Li^+ (pink spheres) and Cl^- (yellow) ions bound. The dark blue mesh represents the spatial distribution of water molecules present in the cation binding pocket for >25% of the simulation time. D1-D1 distances for each snapshot are indicated below each panel.

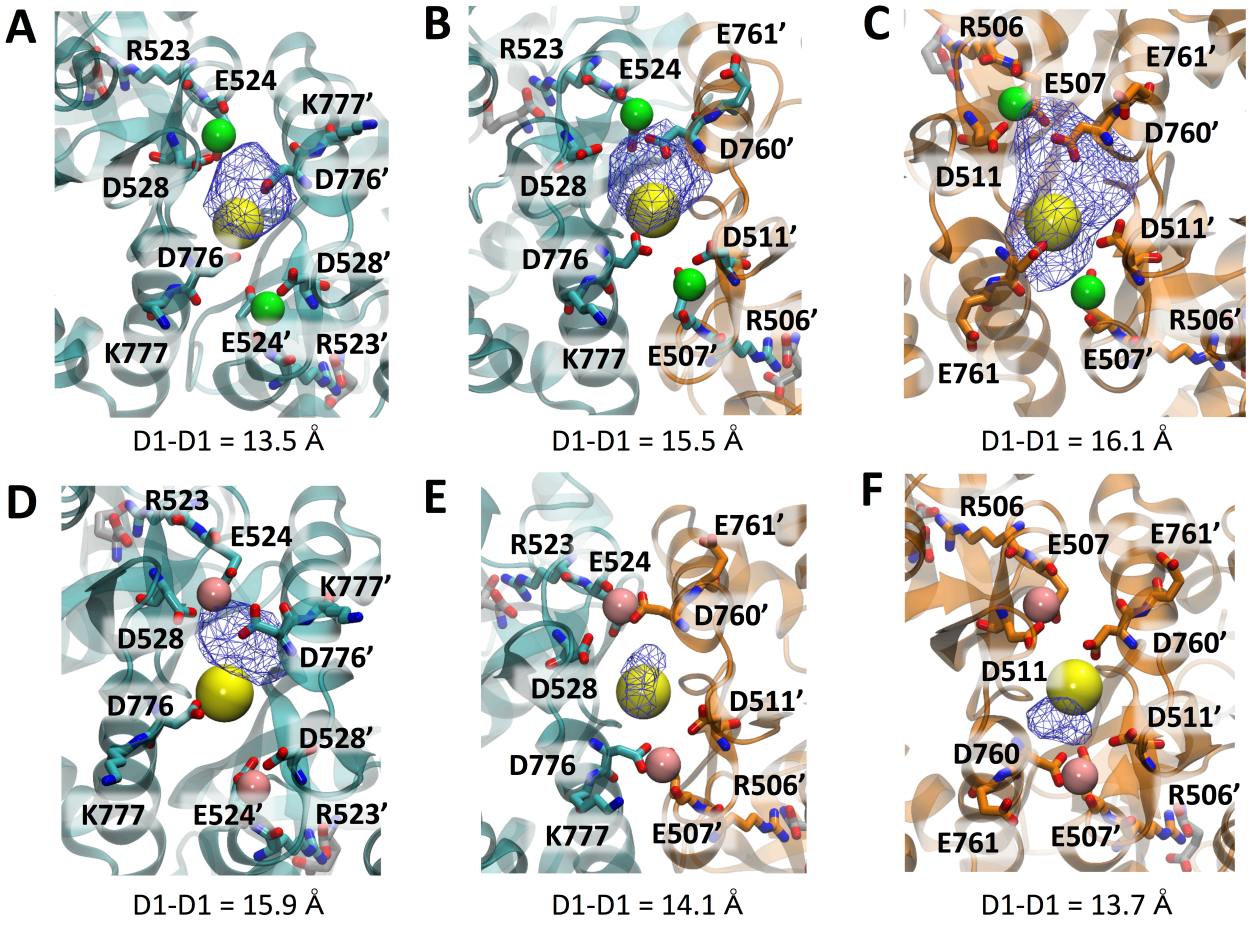

Figure S4: Frequency distribution of the number of ion-dipole interactions between the Li^+ (pink) or Na^+ (green) ions and the solvent in the three LBD systems during 100 ns simulation.

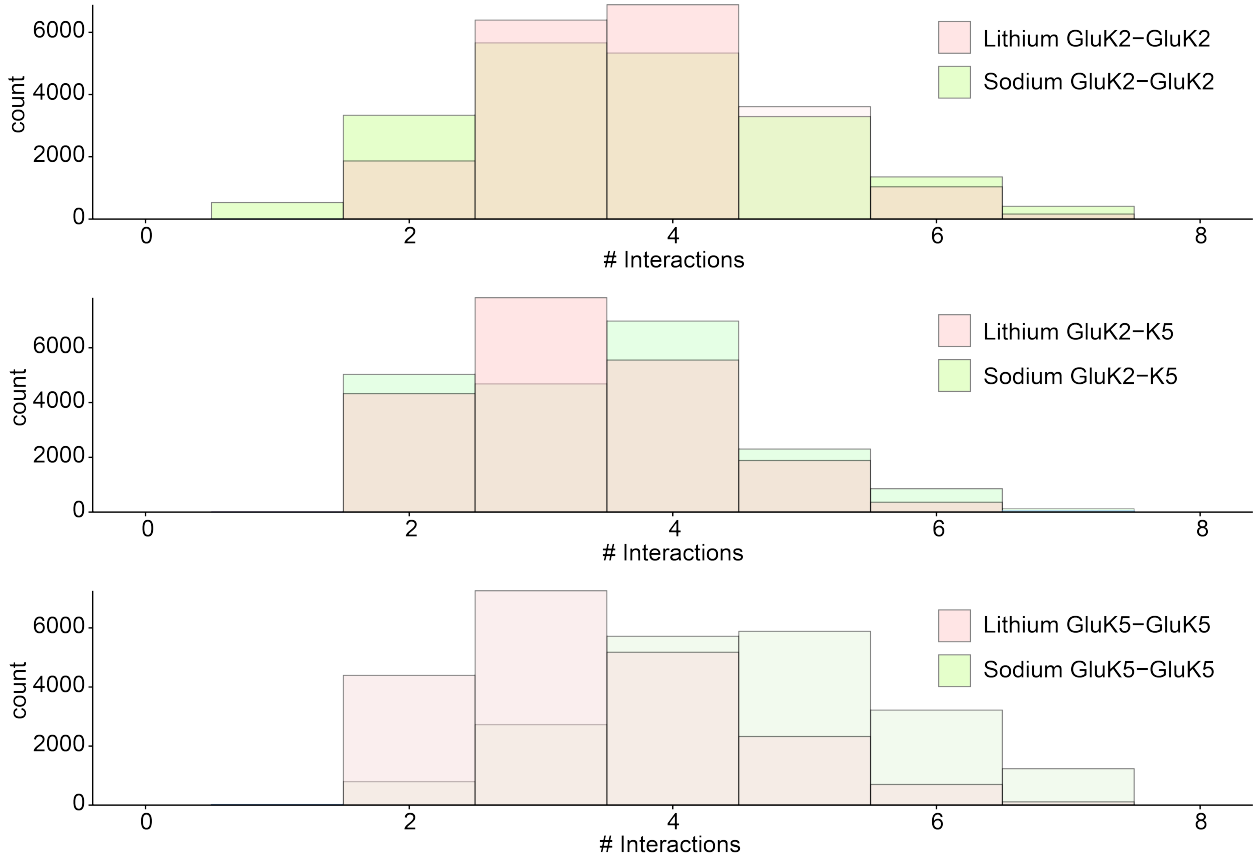

Table S1: Summary of free energy perturbation calculations.

System	Transformation	ΔG (kcal/mol)	Mean Absolute ΔG (kcal/mol)
GluK2/K2	$Na^+ \rightarrow Li^+$	-56.70 ± 0.05	56.52
GluK2/K2	$Li^+ \rightarrow Na^+$	56.33 ± 0.05	
GluK2/K5	$Na^+ \rightarrow Li^+$	-58.82 ± 0.08	59.99
GluK2/K5	$Li^+ \rightarrow Na^+$	61.16 ± 0.02	

The ΔΔG between GluK2/K2 and GluK2/K5 = 3.37 kcal/mol.

References

1. Eswar, N., B. Webb, M. A. Marti-Renom, M. S. Madhusudhan, D. Eramian, M.-y. Shen...,A. Sali. 2006. Comparative protein structure modeling using Modeller. In Current Protocols in Bioinformatics. John Wiley & Sons, Inc.
2. Chaudhry, C., M. C. Weston, P. Schuck, C. Rosenmund, and M. L. Mayer. 2009. Stability of ligand-binding domain dimer assembly controls kainate receptor desensitization. *EMBO J.* 28:1518-1530.
3. Kuusinen, A., M. Arvola, and K. Keinanen. 1995. Molecular dissection of the agonist binding site of an AMPA receptor. *EMBO J.* 14:6327-6332.
4. Traynelis, S. F., L. P. Wollmuth, C. J. McBain, F. S. Menniti, K. M. Vance, K. K. Ogden...,R. Dingledine. 2010. Glutamate receptor ion channels: structure, regulation, and function. *Pharmacol. Rev.* 62:405-496.
5. Laskowski, R. A., M. W. Macarthur, D. S. Moss, and J. M. Thornton. 1993. PROCHECK - A program to check the stereochemical quality of protein structures. *J. Appl. Crystall.* 26:283-291.
6. Benkert, P., M. Kunzli, and T. Schwede. 2009. QMEAN server for protein model quality estimation. *Nucleic Acids Res*.
7. Benkert, P., M. Biasini, and T. Schwede. 2011. Toward the estimation of the absolute quality of individual protein structure models. *Bioinformatics* 27:343-350.
8. Russell, R. B., and G. J. Barton. 1992. Multiple protein sequence alignment from tertiary structure comparison: Assignment of global and residue confidence levels. *Proteins Struct. Funct. Bioinform.* 14:309-323.
9. Humphrey, W., A. Dalke, and K. Schulten. 1996. VMD - Visual molecular dynamics. *J. Mol. Graph.* 14:33-38.
10. Musgaard, M., and P. C. Biggin. 2016. Steered molecular dynamics simulations predict conformational stability of glutamate receptors. *J. Chem. Inf. Model.* 56:1787-1797.
11. Dawe, G. B., M. Musgaard, E. D. Andrews, B. A. Daniels, M. R. P. Aurousseau, P. C. Biggin, and D. Bowie. 2013. Defining the structural relationship between kainate-receptor deactivation and desensitization. *Nat. Struct. Mol. Biol.* 20:1054-1061.
12. Sindhikara, D. J., S. Kim, A. F. Voter, and A. E. Roitberg. 2009. Bad seeds sprout perilous dynamics: Stochastic thermostat induced trajectory synchronization in biomolecules. *J. Chem. Theor. Comput.* 5:1624-1631.
13. Abraham, M. J., T. Murtola, R. Schulz, S. Páll, J. C. Smith, B. Hess, and E. Lindahl. 2015. GROMACS: High performance molecular simulations through multi-level parallelism from laptops to supercomputers. *SoftwareX* 1–2:19-25.
14. Kaminski, G. A., R. A. Friesner, J. Tirado-Rives, and W. L. Jorgensen. 2001. Evaluation and reparametrization of the OPLS-AA force field for proteins via comparison with accurate quantum chemical calculations on peptides. *J. Phys. Chem. B* 105:6474-6487.
15. Vijayan, R., A. J. R. Plested, M. L. Mayer, and P. C. Biggin. 2009. Selectivity and cooperativity of modulatory ions in a neurotransmitter receptor. *Biophys. J.* 96:1751-1760.
16. Jorgensen, W. L., J. Chandresekhar, J. D. Madura, R. W. Impey, and M. L. Klein. 1983. Comparison of simple potential functions for simulating liquid water. *J. Chem. Phys.* 79:926-935.
17. Hess, B., J. Bekker, H. J. C. Berendsen, and J. G. E. M. Fraaije. 1997. LINCS: A linear constraint solver for molecular simulations. *J. Comp. Chem.* 18:1463-1472.

18. Páll, S., and B. Hess. 2013. A flexible algorithm for calculating pair interactions on SIMD architectures. *Comput. Phys. Comms* 184:2641-2650.
19. Essman, U., L. Perera, M. L. Berkowitz, T. Darden, H. Lee, and L. G. Pedersen. 1995. A smooth particle mesh Ewald method. *J. Chem. Phys.* 103:8577-8593.
20. Berendsen, H. J. C., J. P. M. Postma, W. F. van Gunsteren, A. DiNola, and J. R. Haak. 1984. Molecular dynamics with coupling to an external bath. *J. Chem. Phys.* 81:3684-3690.
21. Paramo, T., A. East, D. Garzón, M. B. Ulmschneider, and P. J. Bond. 2014. Efficient characterization of protein cavities within molecular simulation trajectories: trj_cavity. *J. Chem. Theor. Comput.* 10:2151-2164.
22. Shirts, M. R., D. L. Mobley, J. D. Chodera, and V. S. Pande. 2007. Accurate and efficient corrections for missing dispersion interactions in molecular simulations. *J. Phys. Chem. B.* 111:13052-13063.
23. Shirts, M. R., and J. D. Chodera. 2008. Statistically optimal analysis of samples from multiple equilibrium states. *J. Chem. Phys.* 129:124105.
24. Chodera, J. D. 2016. A simple method for automated equilibration detection in molecular simulations. *J. Chem. Theory Comp.* 12:1799-1805.
25. Landes, C. F., A. Rambhadran, J. N. Taylor, F. Salatan, and V. Jayaraman. 2011. Structural landscape of isolated agonist-binding domains from single AMPA receptors. *Nat. Chem. Biol.* 7:168-173.
26. Brown, P. M. G. E., M. Aurousseau, M. Musgaard, P. C. Biggin, and D. Bowie. 2016. Kainate receptor pore-forming and auxiliary subunits regulate channel block by a novel mechanism. *J. Physiol.* 594:1821-1840.